Imino- and Oxazolino-Functionalised Pyrrolylphosphanes and Pyrrolylphosphinites: An Unexploited Class of Chiral *P,N*-Bidentate Ligands with Unusual Electronic Properties

Konstantin N. Gavrilov,[a] Vasily N. Tsarev,*[b] Stanislav I. Konkin,[a] Sergey E. Lyubimov,[b] Alexander A. Korlyukov,[b] Mikhail Yu. Antipin,[b] and Vadim A. Davankov[b]

Keywords: Allylic substitution / Asymmetric catalysis / Palladium / *P,N*-bidentate ligands / Rhodium

Enantiopure *P,N*-bidentate pyrrolylphosphanes and pyrrolylphosphinites have been prepared based upon chiral imino- and oxazolino-containing compounds. Complexation of the new ligands with $[Rh(CO)_2Cl]_2$ and $[Pd(allyl)Cl]_2$ has been found to give the chelate complexes $[Rh(CO)Cl(\eta^2\text{-}P,N)]$ and $[Pd(allyl)(\eta^2\text{-}P,N)]^+BF_4^-$, respectively. Imino- and oxazolino-functionalised pyrrolylphosphanes and pyrrolylphosphinites have been shown to be a novel class of *P,N*-bidentate ligands possessing exceptional π-acceptor and original σ-donor properties. With these ligands, up to 77 % *ee* has been achieved in the asymmetric Pd-catalyzed sulfonylation of 1,3-diphenyl-2-propenyl acetate with sodium *p*-toluenesulfinate. In the enantioselective alkylation of 1,3-diphenyl-2-propenyl acetate with dimethyl malonate, up to 93 % enantioselectivity has been achieved by using $[Pd(allyl)(\eta^2\text{-}P,N)]^+BF_4^-$ complexes as chiral catalysts.

Introduction

In the last decade, (1-pyrrolyl)phosphanes ($PPh_x(NC_4H_4)_{3-x}$, x = 0–2), phosphinites and phosphonites ($P(OPh)_x(NC_4H_4)_{3-x}$, x = 1–2) have been successfully applied in the synthesis of rhodium[1–7] and cobalt[8] complexes, as well as in Rh-catalyzed hydroformylation.[9,10] A set of spectroscopic, structural, and thermochemical measurements[1–7,10] showed that these substances are exceptional π-acceptor ligands. The rationale for this π-acceptor character is best demonstrated by the resonance forms **A**–**D**, Figure 1.

Aromatic delocalisation of the nitrogen lone pair into the five-membered ring places a partial positive charge adjacent to the phosphorus atom. This contribution in **B** and **C** would be expected to render the pyrrolyl substituent an effective electron-withdrawing group. Relative to phenyl, resonance form **D** would also be expected to contribute in an electron-withdrawing fashion, since a more electronegative nitrogen atom replaces carbon.[3] As a result, the substituent parameter χ_i for the 1-pyrrolyl functionality is approximately 12, and the π-acceptor character of these ligands is thus found to exceed that of arylphosphites (–OPh, χ_i = 9.7) and fluorinated aromatic phosphanes (–C_6F_5 χ_i = 11.2).[3]

The higher frequencies of the metal carbonyl stretch for rhodium complexes with pyrrolylphosphanes and pyrrolylphosphonites compared with rhodium complexes with phosphites (Table 1) are consistent with pyrrolyl-based ligands being a better π-acceptor than phosphites, as anticipated from the greater number of 1-pyrrolyl substituents, which reduces the back-donation to the metal carbonyl.

As for σ basicity, the $^1J_{P,Se}$ coupling constants in the ^{31}P NMR spectra of corresponding selenide derivatives indicate

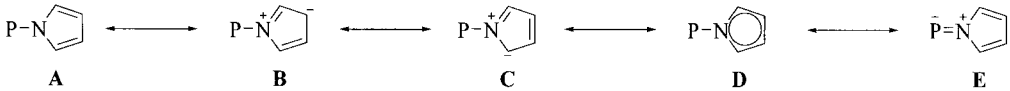

Figure 1. Resonance forms of pyrrolylphosphanes.

[a] Department of Chemistry, Ryazan State Pedagogic University, 46 Svoboda str., Ryazan, 390000, Russia
Fax: +7-0912-775-498
E-mail: chem@ttc.ryazan.ru
[b] Institute of Organoelement Compounds, Russian Academy of Sciences,
28 Vavilova str., Moscow, 119991, Russia
Fax: +7-095-135-6471
E-mail: tsarev@ineos.ac.ru

that $P(NC_4H_4)_3$ ($^1J_{P,Se}$ for $Se{=}P(NC_4H_4)_3$ = 970 Hz) is more basic than $P(OPh)_3$ and constrained phosphites ($^1J_{P,Se}$ for Se=L = 1099–1011 Hz) and less basic than $P(NR_2)_3$ ($^1J_{P,Se}$ for Se=L = 854–784 Hz).[6] For estimating the σ basicity of pyrrolylphosphanes, we suggest a well-known criterion that the values of $^1J_{P,Rh}$ coupling constants in the ^{31}P NMR spectra of corresponding chlorocarbonyl complexes

 DOI: 10.1002/ejic.200500075

Table 1. Spectroscopic data for the complexes [Rh(acac)(CO)L] and *trans*-[RhCl(CO)L_2].

Complex	ν(CO) [cm^{-1}] (CH_2Cl_2)	$^1J_{P,Rh}$, [Hz] ($CDCl_3$)
[Rh(acac)(CO){P(NC_4H_4)$_3$}][5]	2012	251
[Rh(acac)(CO){P(OPh)$_3$}][4,5]	2006	293
[Rh(acac)(CO){P(OEt)$_3$}][11]	1990	267
[Rh(CO){P(NC_4H_4)$_3$}$_2$Cl][1,2]	2024	180
[Rh(CO){P(NC_4H_4)$_2$(OPh)}$_2$Cl][10]	2018	190
[Rh(CO){P(OPh)$_3$}$_2$Cl][2]	2016	210

of rhodium(I) strongly correlate with the s character of the phosphorus lone pair.[11,12] According to this criterion, pyrrolylphosphanes are strong σ bases comparable not only with P(OPh)$_3$ and constrained phosphites, but also with alkyl phosphites (Table 1). A possible reason is a significant contribution of the resonance form with partial negative charge at the phosphorus atom, and easy polarization of the aromatic group.[13] Values of $^1J_{P,Se}$ and $^1J_{P,Rh}$ seem to be more correct criteria for σ basicity than the bond lengths Rh–P used by some authors.[14] On the basis of the X-ray data for the isostructural complexes [Rh(acac)(CO){P(OPh)$_3$}] (Rh–P 2.170 Å) and [Rh(acac)(CO){P(NC_4H_4)$_3$}] (Rh–P 2.166 Å), they made a conclusion about stronger σ-donor properties of P(OPh)$_3$ in comparison to P(NC_4H_4)$_3$. However, bond lengths M–P are dependent not only on σ basicity, but also on π acidity of the ligand.[6] Thus, in another pair of isostructural compounds [Rh(acac){P(OPh)$_3$}$_2$] (Rh–P 2.147, 2.156 Å) and [Rh(acac){P(NC_4H_4)$_3$}$_2$] (Rh–P 2.161, 2.176 Å), bonds Rh–P are longer in the complex with P(NC_4H_4)$_3$,[4] while $^1J_{P,Rh}$ is 291 and 261 Hz, respectively (compare also with the data in Table 1).

Therefore, pyrrolylphosphanes and pyrrolylphosphinites are characterised by rather paradoxical electronic properties, and are both more potent π acids and σ bases than phosphites, representing a novel and efficient group of optically active ligands.[15–17] It should be noted that the –P(NC_4H_4)$_2$ building block and the common chiral ligand –PPh$_2$ fragment are practically the same size, according to their Tolman's cone angle values.[1,4] One could expect that such unusual electronic and steric properties of ligands with –P(NC_4H_4)$_2$ fragments make these compounds promising for asymmetric catalysis, but to the best of our knowledge no examples of their catalytic application are known. In the present communication we report previously unknown chiral pyrrolylphosphanes and pyrrolylphosphinites and pioneering results of their application in the coordination chemistry of palladium and in asymmetric Pd-catalysed allylation.

Results and Discussion

The new *P,N*-bidentate pyrrolylphosphinites **2a**–**c** and pyrrolylphosphanes **2d**,**e** were obtained from chlorobis(1-pyrrolyl)phosphane in one step (Scheme 1).

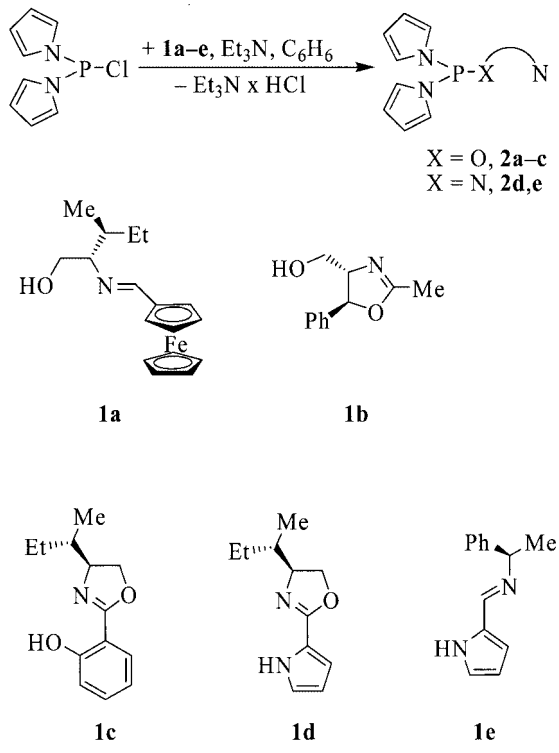

Scheme 1.

Compounds **2a**–**e** are soluble in common nonprotic solvents and stable under dry conditions. Unlike P(NC_4H_4)$_3$, ligands **2d** and **2e** are moisture sensitive. A possible reason for this, as in the case of the keto-functionalised ligand P(NC_4H_4)$_2$(NC_4H_3C(O)Me-2),[7] is that a functionalised pyrrole ring represents a better leaving group than the unfunctionalised pyrrolyl groups and, additionally, is able to form hydrogen bonds with incoming protic nucleophiles.

Using the compounds **2a**–**e**, neutral and cationic *cis*-chelate metal complexes were obtained (Scheme 2).

Some important spectroscopic data of the complexes are summarised in Table 2.

The $^1J_{P,Rh}$ and ν(CO) data for complexes **3a**–**e** are in good agreement with the suggested structures.[18] IR and ^{13}C NMR spectroscopic characteristics of the carbonyl ligands in complexes **3a**–**e** (δ_C = 186.2 ppm, $^1J_{C,Rh}$ = 72 Hz, ^2J(C,P) = 16 Hz for **3a** and δ_C = 184.9 ppm, $^1J_{C,Rh}$ = 68 Hz, $^2J_{C,P}$ = 17 Hz for **3e**) indicate that **2a**–**e** represent a novel group of highly π-accepting *P,N*-bidentate ligands.[4,7,19] Notably, the ν(CO) values of **3d**,**e** prove that

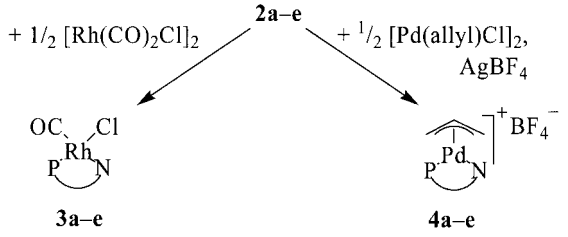

Scheme 2.

Table 2. Selected spectroscopic data for compounds **3a**–**e** and **4a**–**e** (in $CHCl_3$).

Compound	^{31}P NMR Spectroscopy δ_P	^1J(P,Rh) [Hz]	IR Spectroscopy ν(CO) [cm^{-1}]
3a	116.7	242	2032
3b	116.3	242	2034
3c	126.2	256	2036
3d	93.4	245	2039
3e	94.9	249	2040
4a	113.1, 112.6	–	–
4b	115.6, 115.1	–	–
4c	125.5, 124.7	–	–
4d	89.3, 88.8	–	–
4e	92.5	–	–

ligands **2d**,**e** bearing three pyrrole rings, are the most π acidic in the group. A comparison of the $^1J_{P,Rh}$ and ν(CO) data for compounds **3a**–**c** (Table 2) and isostructural rhodium complexes previously described by us[18,20,21] (Table 3)

Table 3. Selected spectral parameters for [Rh(CO)Cl(η^2-*P,N*)] complexes with *P,N*-bidentate arylphosphite ligands.

Ligand	ν(CO), cm^{-1} ($CHCl_3$)	$^1J_{P,Rh}$, Hz ($CHCl_3$)
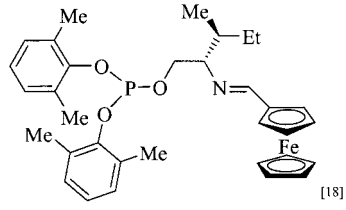 [18]	2025	279
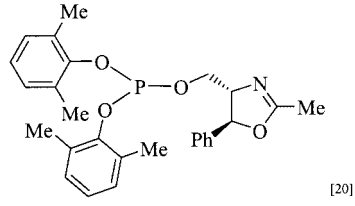 [20]	2030	277
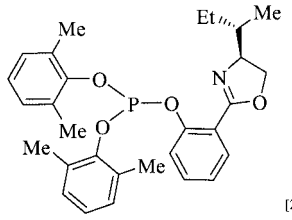 [21]	2024	287

supports a general conclusion about higher σ-donor and π-acceptor properties of pyrrolylphosphanes and pyrrolylphosphinites with respect to phosphites.

It is rather difficult to determine the best σ donor among the ligands **2a**–**e**, since the $^1J_{P,Rh}$ values in chloro carbonyl rhodium chelate complexes depend largely on the nature of a nitrogen-containing fragment (see ref.[18] and references cited therein). But in the case of **3c** and **3d**, the ^{31}P NMR spectroscopic data (Table 2) indicate that pyrrolylphosphane **2d** is a stronger σ donor than pyrrolylphosphinite **2c**.

Complexes **3a**, **3c** and **3d** were characterised by X-ray diffraction. Their molecular structures are shown in Figure 2, Figure 3 and Figure 4, and selected bond lengths and angles are given in Table 4.

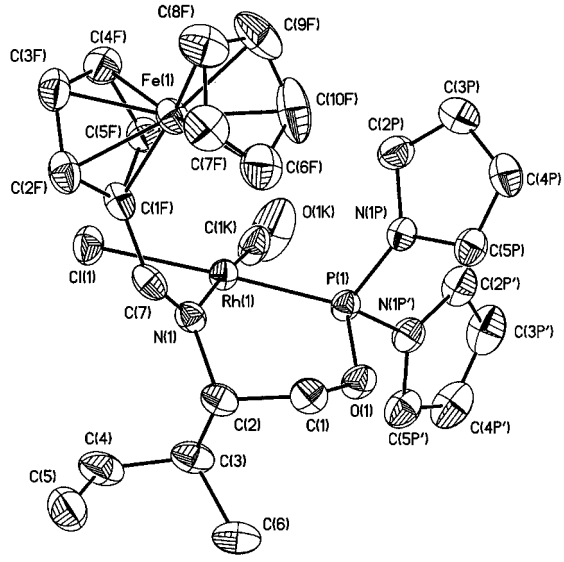

Figure 2. Molecular structure of complex **3a**. Atoms are given by thermal ellipsoids at 50% probability. Principal bonds and angles (Å and °): Rh(1)–C(1K) 1.837(3), Rh(1)–N(1) 2.141(2), Rh(1)–P(1) 2.1576(8), Rh(1)–Cl(1) 2.3742(9), P(1)–O(1) 1.598(2), P(1)–N(1P) 1.691(2), P(1)–N(1P′) 1.703(2), O(1)–C(1) 1.444(3), O(1K)–C(1K) 1.134(4); O(1)–P(1)–N(1P) 103.34(12), O(1)–P(1)–N(1P′) 96.27(12), N(1P)–P(1)–N(1P′) 100.49(11), O(1)–P(1)–Rh(1) 116.68(8), N(1P)–P(1)–Rh(1) 116.72(8), N(1P′)–P(1)–Rh(1) 119.95(9).

From X-ray studies it was found that in the crystal the molecules of **3a**,**c**,**d** are characteried by *S* configurations of C(2) and C(3) for **3a**, C(4) and C(5) for **3c**, and C(4) and C(5) for the **3d** asymmetric atoms, respectively.

The distorted sofa conformation (the deviation of the P(1) atom from the basal plane is 0.81 Å) of the six-membered metallacycle is observed in compound **3d**. In compound **3a,** where the fused five-membered cyclic fragments are absent, the six-membered metallacycle adopts the distorted chair conformation with deviations of the P(1) and C(2) atoms by 0.57 and 0.79 Å, respectively. The chair conformation of the six-membered metallacycle is also observed in previously studied complexes with the 1,3-diaza-2-phosphabicyclo[3.3.0]octane ligand.[22] So, it can be concluded that the distorted sofa conformation in **3d** is caused by the presence of five-membered cycles fused with the metallacycle.

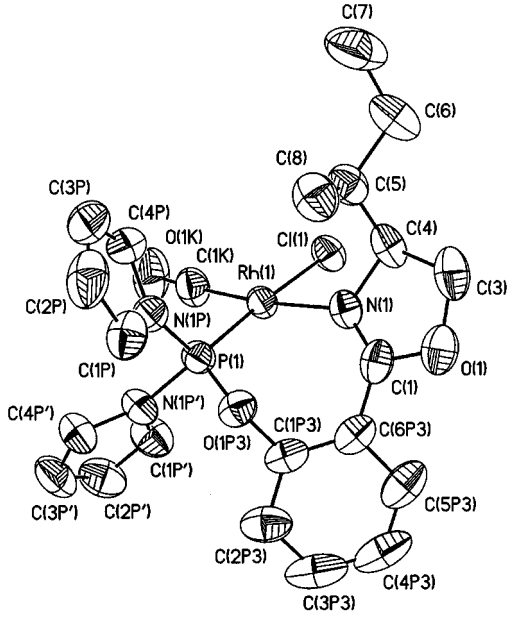

Figure 3. Molecular structure of complex **3c**. Atoms are given by thermal ellipsoids at 50% probability. Principal bonds and angles (Å and °): Rh(1)–C(1K) 1.828(3), Rh(1)–N(1) 2.1020(19), Rh(1)–P(1) 2.1553(9), Rh(1)–Cl(1) 2.3810(9), P(1)–O(1P3) 1.6166(17), P(1)–N(1P) 1.691(2), P(1)–N(1P′) 1.696(2), O(1K)–C(1K) 1.134(3); O(1P3)–P(1)–N(1P) 94.72(10), O(1P3)–P(1)–N(1P′) 103.95(10), N(1P)–P(1)–N(1P′) 102.73(10), O(1P3)–P(1)–Rh(1) 116.33(6), N(1P)–P(1)–Rh(1) 119.85(8), N(1P′)–P(1)–Rh(1) 116.05(8).

The seven-membered metallacycle in **3c** is fused with phenyl and oxazoline moieties and its conformation may be described as a distorted boat. Atoms C(1P3), C(6P3) and Rh(1) deviate from the plane P(1)O(1P3)N(1)C(1) by 0.93, 0.98 and 0.68 Å, respectively.

Table 4. Selected bond lengths [Å] and angles [°] for complexes **3a**, **3c** and **3d**.

	3a	**3c**	**3d**
Rh(1)–C(1K)	1.837(3)	1.828(3)	1.838(3)
Rh(1)–N(1)	2.141(2)	2.1019(19)	2.111(2)
Rh(1)–P(1)	2.158(1)	2.155(1)	2.145(1)
Rh(1)–Cl(1)	2.374(1)	2.381(1)	2.363(1)
O(1K)–C(1K)	1.134(4)	1.134(3)	1.129(4)
N(1)–Rh(1)–P(1)	88.36(7)	90.20(6)	86.54(6)
C(1K)–Rh(1)–P(1)	89.81(9)	91.13(9)	93.67(10)
C(1K)–Rh(1)–Cl(1)	89.00(9)	89.48(9)	89.35(10)
N(1)–Rh(1)–Cl(1)	92.67(7)	89.64(6)	90.64(6)
P(1)–Rh(1)–Cl(1)	177.35(3)	176.05(2)	174.45(3)
O(1K)–C(1K)–Rh(1)	178.0(3)	176.9(3)	178.1(3)

The oxazoline cycles in **3c** and **3d** have different conformations. In the former case this cycle is planar, while in the latter it adopts the envelope conformation with deviation of the C(4) atom by 0.15 Å. The ferrocenyl substituent in **3a** occupies a pseudoequatorial position.

The *endo*-cyclic rhodium atom has an almost ideal square-planar geometry, its deviation from the basal plane does not exceed 0.02 Å. On the other hand in **4** the deviation of the Rh^{I} atom from the basal plane is more pronounced (0.06 Å), which may be explained by steric overcrowding of the six-membered metallacycle. The P(1)–Rh(1) bonds in **3a**,**c**,**d** are somewhat shorter than those in the previously investigated 1,3-diaza-2-phosphabicyclo[3,3,0]octane ligand complex[22]. On the other hand, the shortening of the P(1)–Rh(1) bond did not lead to respective elongation of the Rh(1)–Cl(1) bond in comparison to the analogous bond in the previously described complex.[22] So, the *trans*-effect of a $P(C_4H_4N)_3$ moiety is almost the same as

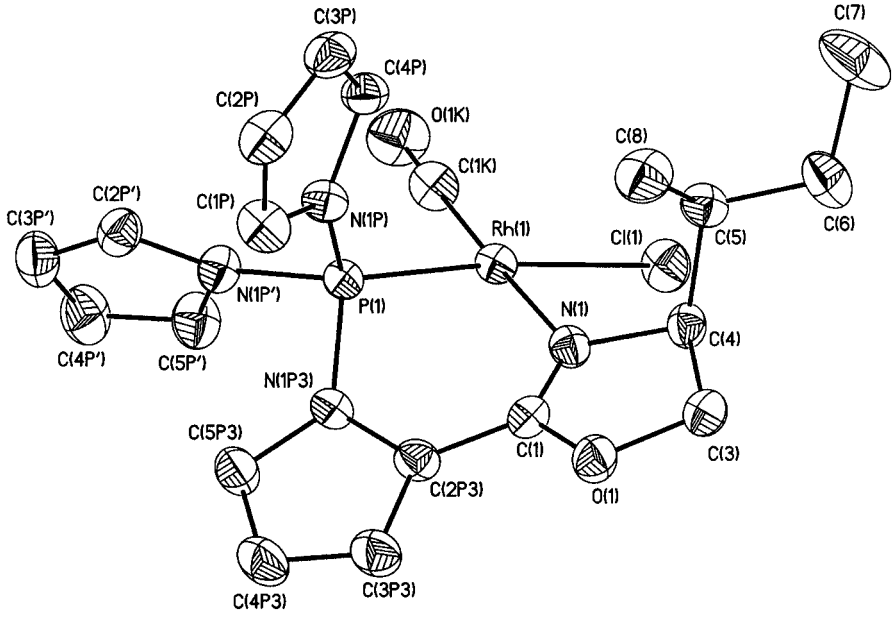

Figure 4. Molecular structure of complex **3d**. Atoms are given by thermal ellipsoids at 50% probability. Principal bonds and angles (Å and °): Rh(1)–C(1K) 1.838(3), Rh(1)–N(1) 2.111(2), Rh(1)–P(1) 2.1448(8), Rh(1)–Cl(1) 2.3631(9), P(1)–N(1P) 1.681(2), P(1)–N(1P′) 1.698(2), P(1)–N(1P3) 1.717(2), C(1K)–O(1K) 1.129(4); N(1P)–P(1)–N(1P′) 102.52(12), N(1P)–P(1)–N(1P3) 99.87(12), N(1P′)–P(1)–N(1P3) 100.44(11), N(1P)–P(1)–Rh(1) 118.26(8), N(1P′)–P(1)–Rh(1) 121.83(9), N(1P3)–P(1)–Rh(1) 110.46(8).

in the case of the 1,3-diaza-2-phosphabicyclo[3.3.0]octane fragment.

The geometry of the P(1) atom in **3a** and **3c** is distorted tetrahedral, the bond angles at this atom vary in the range of 94–119°. It should be noted that endocyclic P–O bonds in **3a**,**c**,**d** have almost the same lengths as in previously studied compound.[22]

There is no correlation between $^1J_{P,Rh}$ values and Rh–P bond lengths, because, as mentioned above, the Rh–P bond length depends not only on σ basicity but also on the π acidity of the P ligand. Thus, the shortest Rh–P bonds were found in the complexes with the most π-acceptor pyrrolylphosphanes [Rh(CO)($P(NC_4H_4)_2(NC_4H_3C(O)Me$-2))Cl] [2.147 Å, $^1J_{P,Rh}$ = 237 Hz, $\tilde{\nu}$(CO) = 2017 cm^{-1} (KBr)],[7] [Rh(CO)($P(NC_4H_4)_2$(7-aza-1-indolyl))Cl] and **3d** (Table 5); **3d** has the shortest Rh–P bond among these complexes and related compounds like [Rh(acac)(CO){$P(NC_4H_4)_3$}]. The data in Table 5 clearly demonstrate that *ν*(CO) in the IR spectra of [Rh(CO)(L)Cl] complexes is strongly affected by changings in the π acidity of *P,N*-bidentate ligands. In particular, pyrrolylphosphane $P(NC_4H_4)_2$(7-aza-1-indolyl) is a much stronger π acceptor than $P(Ph)_2$(7-aza-1-indolyl), but weaker than **2d**,**e**. It is notable that whereas *ν*(CO) for the rhodium complexes varies significantly from 1986 to 2040 cm^{-1} ($\Delta\tilde{\nu}$(CO) = 54 cm^{-1}), $\Delta^1J_{C,Rh}$ does not exceed a mere 6 Hz (Table 5). Moreover, the $\tilde{\nu}$(CO) magnitudes of [Rh(CO)($P(Ph)_2$(7-aza-*N*-indolyl))Cl] and [Rh(CO)-($P(NC_4H_4)_2$(7-aza-*N*-indolyl)Cl] differ by 22 cm^{-1}, while their $^1J_{C,Rh}$ values are equal. These facts are in good agreement with a conclusion made earlier by us that $^1J_{C,Rh}$ for *cis-P,N*-chelate chlorocarbonyl complexes [Rh(CO)(L)Cl] lie within a narrow interval of 68–75 Hz and are practically indifferent to electronic characteristics of a phosphorus atom environment.[20] Duplication of peaks in the ^{31}P NMR spectra of compounds **4a**–**d** (Table 2) indicates the presence of their *exo*- and *endo*-isomers.[18,21] Sharp singlets in the ^{31}P NMR spectrum of **4e** can be rationalised either by fast interconversion of the isomers or by an absence of one of them.

Pyrrolylphosphanes and pyrrolylphosphinites **2a**–**e** and complexes **4c**,**d** were tested in asymmetric Pd-catalysed allylic substitution reactions (Scheme 3).

The results of allylic sulfonylation are summarised in Table 6. Good optical (up to 77% *ee*) and moderate chemi-

Table 5. Some spectral and structural parameters of *cis-P,N*-chelate chlorocarbonyl complexes [Rh(CO)(L)Cl].

Ligand	ν(CO), cm^{-1} ($CHCl_3$)	$^1J_{P,Rh}$ ($^2J_{C,P}$), Hz ($CDCl_3$)	$^1J_{P,Rh}$, Hz ($CHCl_3$)	Rh–P, Å
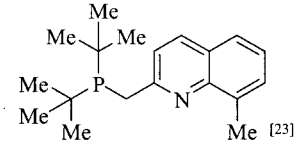 [23]	1986	74 (21)	167	–
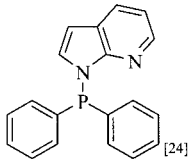 [24]	2005	70 (23)	180	2.198
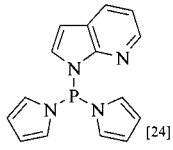 [24]	2027	70 (23)	242	2.165
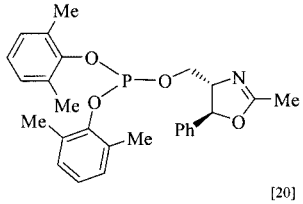 [20]	2030	72 (19)	277	2.173
2a	2032	72 (16)	242	2.158
2c	2036	–	256	2.155
2d	2039	–	245	2.145
2e	2040	68 (17)	249	–

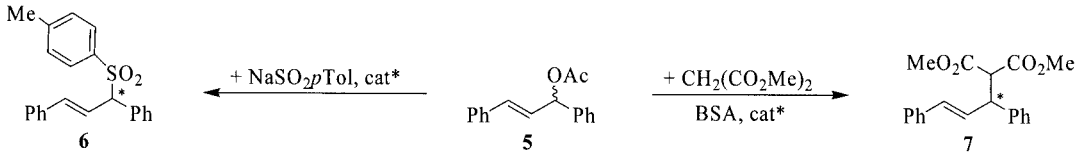

Scheme 3.

cal (up to 60%) yields of product **6** were achieved. **2b** (entry 5) was found to be the most stereoselective ligand, while **2a**, **2c** and **2e** showed basically the same enantioselectivity (54–64%), and no conversion was observed with **2d** (entries 10–12). An increased L*/Pd molar ratio in the processes catalysed by $[Pd(allyl)Cl]_2$ resulted in higher optical and chemical yields (entries 1,2; 4,5). Worth noting is that the most successful catalyst precursor for **2c** happened to be $[Pd_2(dba)_3]\times CHCl_3$ (entries 7–9).

Table 6. Enantioselective allylic sulfonylation of **5** with $NaSO_2pTol$ (in THF).

Entry	Catalyst precursor	Ligand	L*/Pd	Isolated yield [%]	*ee* [%][a]
1	$[Pd(allyl)Cl]_2$	**2a**	1:1	17	32 (*R*)
2	$[Pd(allyl)Cl]_2$	**2a**	2:1	60	64 (*R*)
3	$[Pd_2(dba)_3]\times CHCl_3$	**2a**	1:1	16	33 (*R*)
4	$[Pd(allyl)Cl]_2$	**2b**	1:1	0	–
5	$[Pd(allyl)Cl]_2$	**2b**	2:1	26	77 (*R*)
6	$[Pd_2(dba)_3]\times CHCl_3$	**2b**	1:1	15	15 (*S*)
7	$[Pd(allyl)Cl]_2$	**2c**	1:1	37	7 (*S*)
8	$[Pd(allyl)Cl]_2$	**2c**	2:1	30	7 (*S*)
9	$[Pd_2(dba)_3]\times CHCl_3$	**2c**	1:1	25	54 (*S*)
10	$[Pd(allyl)Cl]_2$	**2d**	1:1	0	–
11	$[Pd(allyl)Cl]_2$	**2d**	2:1	0	–
12	$[Pd_2(dba)_3]\times CHCl_3$	**2d**	1:1	0	–
13	$[Pd(allyl)Cl]_2$	**2e**	1:1	22	57 (*R*)
14	$[Pd(allyl)Cl]_2$	**2e**	2:1	31	58 (*R*)

[a] *ee* measured by HPLC [(*R*,*R*)-Whelk-01, hexane/*i*PrOH = 4:1, 1 mL/min, 254 nm].

For the asymmetric allylic alkylation (Scheme 3, Table 7), ligands **2a** and **2c** provided the best results (entries 1,2,5). Thus, cationic complex **4c** afforded the product in 93% *ee* (93% conversion, entry 7).

Table 7. Enantioselective allylic alkylation of **5** with dimethyl malonate (in THF, L*/Pd = 1:1).

Entry	Catalyst	Conv. [%][a]	*ee* [%][b]
1	$[Pd(allyl)Cl]_2$/**2a**	99	83 (*R*)
2	$[Pd_2(dba)_3]\times CHCl_3$/**2a**	91	81 (*R*)
3	$[Pd(allyl)Cl]_2$/**2b**	99	44 (*R*)
4	$[Pd_2(dba)_3]\times CHCl_3$/**2b**	99	38 (*R*)
5	$[Pd(allyl)Cl]_2$/**2c**	46	88 (*S*)
6	$[Pd_2(dba)_3]\times CHCl_3$/**2c**	12	61 (*S*)
7	**4c**	93	93 (*S*)
8	$[Pd(allyl)Cl]_2$/**2d**	19	64 (*S*)
9	$[Pd_2(dba)_3]\times CHCl_3$/**2d**	8	36 (*R*)
10	**4d**	0	–
11	$[Pd(allyl)Cl]_2$/**2e**	11	80 (*S*)
12	$[Pd_2(dba)_3]\times CHCl_3$/**2e**	10	67 (*S*)

[a] Measured by HPLC. [b] Determined by HPLC (Daicel Chiralcel OD-H, hexane/*i*PrOH = 99:1; 0.5 mL/min, 254 nm).

Stereoinduction of pyrrolylphosphane **2e** is close to **2a** and **2c** (entry 11), but conversion is low. Ligands **2b** and **2d** demonstrated moderate enantioselectivity (up to 64% *ee*) with substantially low conversion in the case of **2d**. In contrast to allylic sulfonylation, $[Pd(allyl)Cl]_2$ was a superior catalyst precursor for all ligands.

Conclusions

Several chiral imino- and oxazolino-functionalised pyrrolylphosphanes and pyrrolylphosphinites were obtained for the first time by a simple one-step synthesis. These compounds have been shown to be a novel class of *P,N*-bidentate ligands possessing exceptional π-acceptor and original σ-donor properties. The new ligands were used in asymmetric Pd-catalyzed allylic substitution where up to 93% *ee* was achieved in the benchmark test with 1,3-diphenyl-2-propenyl acetate and dimethyl malonate. It should be pointed out, however, that the present work describes only five substances in this general class. A tremendous variety of similar substituents such as substituted pyrroles, indoles, imidazoles, pyrazoles, etc., are commercially available or obtainable by synthetic means.[1] The simple synthesis of pyrrolylphosphanes and pyrrolylphosphinites, their outstanding electronic properties, together with the wide variety of accessible pyrrolelike precursors make it an attractive area of research with great promise.

Experimental Section

General Remarks: All reactions were performed under argon in dehydrated solvents. IR spectra were recorded with a Specord M80 instrument. ^{31}P and ^{13}C NMR spectra were recorded with a Bruker AMX 400 instrument (162.0 MHz for ^{31}P, 100.6 MHz for ^{13}C). The assignments of the signals in the ^{13}C NMR spectra were made with the use of the DEPT technique and, for pyrrolyl substituents, using literature data.[10] Chemical shifts (ppm) are given relative to Me_4Si (^{13}C NMR) and 85% H_3PO_4 (^{31}P NMR). Mass spectra were recorded with a Kratos MS890 spectrometer (EI), an MSVKh TOF spectrometer with ionization by Cf-252 fission fragments (plasma desorption technique, PD) and AMD 402 spectrometer (FAB). Optical rotations were measured on a Perkin–Elmer 141 polarimeter. Elemental analyses were performed at the Laboratory of Microanalysis (Institute of Organoelement Compounds, Moscow).

$[Rh(CO)_2Cl]_2$,[25] $[Pd(allyl)Cl]_2$,[26] $[Pd_2(dba)_3]\times CHCl_3$,[27] chlorobis(1-pyrrolyl)phosphane,[10] compounds **1a**,[18] **1c**,[28] **1d**[29] and **1e**[30] were synthesised using literature procedures. 4-Hydroxymethyl-2-methyl-5-phenyl-2-oxazoline (**1b**) was purchased from Fluka. The syntheses of rhodium(I) complexes **3a**–**e** and palladium(II) complexes **4a**–**e** were performed by techniques similar to that reported.[18,31]

$NaSO_2pTol$, $CH_2(CO_2Me)_2$ and *N*,*O*-bis(trimethylsilyl)acetamide (BSA) were purchased from Acros Organics. Compound **5** was syn-

thesised as published.[26] The catalytic experiments were carried out according to published procedures.[22]

Preparation of Ligands. General Technique: A solution of chlorobis(1-pyrrolyl)phosphane (4.2×10^{-3} mol) in benzene (15 mL) was added dropwise to a stirred solution of the appropriate compound **1a**–**e** (4.2×10^{-3} mol) and Et_3N (0.6 mL, 4.2×10^{-3} mol) in the same solvent (15 mL) at 0 °C. The reaction mixture was then heated to boiling point, allowed to cool down, stirred for 0.5 h at 50 °C, allowed to cool to room temperature and filtered. The solvent was removed in vacuo (40 Torr), and the residue was concentrated and dried in vacuo (1 Torr, 2 h).

{(2*S*)-2-(Ferrocenylmethylideneamino)-2-[(1*S*)-1-methylpropyl]-ethoxy}bis(1-pyrrolyl)phosphinite (2a): Yield: 1.85 g, 93%; dark red oil. $[a]_D^{21}$ = +151.4 (*c* = 0.5, $CHCl_3$). ^{13}C NMR ($CDCl_3$): δ_C = 161.7 (CH=N), 121.1 (d, ^2J = 14.9 H, CHNP), 120.9 (d, ^2J = 14.7 Hz, CHNP), 111.7 (d, ^3J = 6.5 Hz, *C*HCHNP), 111.6 (d, ^3J = 6.1 Hz, *C*HCHNP), 80.4 [$C_{Fc(ipso)}$], 76.3 (d, ^3J = 5.3 Hz, CHN), 70.1, 69.9, 69.1, 67.5 (all C_{Fc}), 69.2 (d, ^2J = 16.3 Hz, CH_2OP), 68.7 (C_{Cp}), 36.1 (*C*HCH$_3$), 25.2 (*C*H$_2$CH$_3$), 15.7 (CH*C*H$_3$), 10.8 (CH$_2$*C*H$_3$) ppm. ^{31}P NMR ($CDCl_3$): δ_P = 113.6 ppm. MS (70 eV, EI): *m*/*z* (%): 475 (6) $[M]^+$, 409 (64) [M – pyrrolyl]$^+$, 264 (95), 121 (100). MS (PD): *m*/*z* (%): 475 (80) $[M]^+$, 409 (100) [M – pyrrolyl]$^+$. MS (FAB): *m*/*z* (%): 475 (16) $[M]^+$, 409 (85) [M – pyrrolyl]$^+$, 264 (100). Elemental analysis for $C_{25}H_{30}FeN_3OP$ (475.2): calcd. C 63.17, H 6.36, N 8.84; found C 63.31, H 6.29, N 8.71.

[(4*S*,5*S*)-(2-Methyl-5-phenyl-2-oxazolin-4-yl)methoxy]bis(1-pyrrolyl)phosphinite (2b): Yield 1.33 g, 90%; light yellow oil. $[a]_D^{21}$ = –158.3 (*c* = 1, $CHCl_3$). ^{13}C NMR ($CDCl_3$): δ_C = 166.0 (C=N), 139.8, 128.5, 128.1, 125.1 (all C_{Ph}), 121.0 (d, ^2J = 10.3 Hz, CHNP), 120.9 (d, ^2J = 10.1 Hz, CHNP), 111.9 (d, ^3J = 5.3 Hz, *C*HCHNP), 111.8 (d, ^3J = 5.0 Hz, *C*HCHNP), 82.6 (CHO), 74.6 (d, ^3J = 6.5 Hz, CHN), 68.3 (d, ^2J = 18.3 Hz, CH_2OP), 13.5 (CH_3) ppm. ^{31}P NMR ($CDCl_3$): δ_P = 114.5 ppm. MS (PD): *m*/*z* (%): 353 (7) $[M]^+$, 313 (55), 101 (100). MS (FAB): *m*/*z* (%): 353 (2) $[M]^+$, 287 (100) [M – pyrrolyl]$^+$, 182 (83). Elemental analysis for $C_{19}H_{20}N_3O_2P$ (353.1): calcd. C 64.58, H 5.70, N 11.89; found C 64.39, H 5.77, N 12.01.

{2-[(4*S*)-4-*sec*-Butyl-2-oxazolin-2-yl]phenoxy}bis(1-pyrrolyl)phosphinite (2c): Yield 1.46 g, 92%; light yellow oil. $[a]_D^{21}$ = –17.5 (*c* = 1, $CHCl_3$). ^{13}C NMR ($CDCl_3$): δ_C = 160.6 (C=N), 151.4 (d, ^2J = 10.3 Hz), 132.0, 130.9, 124.4, 120.6, 116.4 (all C_{Ar}), 121.6 (d, ^2J = 15.9 Hz, CHNP), 121.5 (d, ^2J = 16.4 Hz, CHNP), 111.9 (d, ^3J = 5.0 Hz, *C*HCHNP), 111.8 (d, ^3J = 4.6 Hz, *C*HCHNP), 71.3 (CHN), 69.1 (CH_2O), 38.8 (*C*HCH$_3$), 25.7 (*C*H$_2$CH$_3$), 14.2 (CH*C*H$_3$), 11.2 (CH$_2$*C*H$_3$) ppm. ^{31}P NMR ($CDCl_3$): δ_P = 107.6 ppm. MS (PD): *m*/*z* (%): 381 (7) $[M]^+$, 315 (49) [M – pyrrolyl]$^+$, 217 (100). Elemental analysis for $C_{21}H_{24}N_3O_2P$ (381.2): calcd. C 66.13, H 6.34, N 11.02; found C 66.38, H 6.29, N 11.11.

{2-[(4*S*)-4-*sec*-Butyl-2-oxazolin-2-yl]-(1-pyrrolyl)}bis(1-pyrrolyl)-phosphane (2d): Yield 1.32 g, 89%; light orange oil. $[a]_D^{21}$ = –36.1 (*c* = 1, $CHCl_3$). ^{13}C NMR ($CDCl_3$): δ_C = 156.7 (C=N), 126.4 (d, ^2J = 3.8 Hz), 124.7 (d, ^2J = 8.7 Hz), 117.3, 111.7 (all C_{Pyr}), 122.6 (d, ^2J = 15.2 Hz, CHNP), 122.2 (d, ^2J = 14.4 Hz, CHNP), 112.4 (d, ^3J = 4.2 Hz, *C*HCHNP), 112.2 (d, ^3J = 4.2 Hz, *C*HCHNP), 71.3 (CHN), 69.9 (CH_2O), 39.1 (*C*HCH$_3$), 25.4 (*C*H$_2$CH$_3$), 14.3 (CH*C*H$_3$), 11.2 (CH$_2$*C*H$_3$) ppm. ^{31}P NMR ($CDCl_3$): δ_P = 71.9 ppm. MS (PD): *m*/*z* (%): 354 (12) $[M]^+$, 288 (36) [M – pyrrolyl]$^+$, 193 (100). Elemental analysis for $C_{19}H_{23}N_4OP$(354.2): calcd. C 64.39, H 6.54, N 15.81; found C 64.12, H 6.63, N 15.96.

{2-[(1*R*)-1-Phenylethyliminomethyl]-(1-pyrrolyl)}bis(1-pyrrolyl)phosphane (2e): Yield 1.31 g, 87%; red oil. $[a]_D^{21}$ = +68.0 (*c* = 0.8, $CHCl_3$). ^{13}C NMR ($CDCl_3$): δ_C = 148.8 (CH=N), 144.8, 128.2, 126.5, 126.3 (all C_{Ph}), 134.7 (d, ^2J = 2.7 Hz), 126.6 (d, ^2J = 4.2 Hz), 118.5, 112.1 (all C_{Pyr}), 122.5 (d, ^2J = 14.4 Hz, CHNP), 122.2 (d, ^2J = 14.0 Hz CHNP), 112.0 (d, ^3J = 3.8 Hz, *C*HCHNP), 111.8 (d, ^3J = 3.8 Hz, *C*HCHNP), 68.6 (CHN), 24.7 (CH_3) ppm. ^{31}P NMR ($CDCl_3$): δ_P = 68.7 ppm. MS (FAB): *m*/*z* (%): 360 (8) $[M]^+$, 294 (44) [M – pyrrolyl]$^+$, 105 (100). Elemental analysis for $C_{21}H_{21}N_4P$ (360.2): calcd. C 69.99, H 5.87, N 15.55; found C 70.23, H 5.78, N 15.63.

Rhodium Complexes

[Rh(CO)(2a)Cl] (3a): Yield 0.22 g, 94%; red powder; m.p. 215–216 °C (dec.). ^{13}C NMR ($CDCl_3$): δ_C = 171.8 (CH=N), 121.9 (CHNP), 113.1 (*C*HCHNP), 81.0 [$C_{Fc(ipso)}$], 76.1 (CHN), 73.3, 73.1, 72.8, 72.1 (all C_{Fc}), 70.9 (CH_2OP), 69.7 (C_{Cp}), 36.9 (*C*HCH$_3$), 25.2 (*C*H$_2$CH$_3$), 14.3 (CH*C*H$_3$), 10.3 (CH$_2$*C*H$_3$) ppm. IR (KBr): $\tilde{\nu}$(CO) = 2019 cm^{-1}. Elemental analysis for $C_{26}H_{30}ClFeN_3O_2PRh$ (641.0): calcd. C 48.66, H 4.71, N 6.55; found C 48.83, H 4.62, N 6.68.

[Rh(CO)(2b)Cl] (3b): Yield 0.17 g, 90%; light-brown powder; m.p. 208–210 °C (dec.). IR (KBr): $\tilde{\nu}$(CO) = 2016 cm^{-1}. Elemental analysis for $C_{20}H_{20}ClN_3O_3PRh$ (519.0): calcd. C 46.22, H 3.88, N 8.09; found C 46.41, H 3.72, N 7.90.

[Rh(CO)(2c)Cl] (3c): Yield 0.18 g, 89%; orange powder; m.p. 199–200 °C (dec.). IR (KBr): $\tilde{\nu}$(CO) = 2022 cm^{-1}. Elemental analysis for $C_{22}H_{24}ClN_3O_3PRh$ (547.0): calcd. C 48.24, H 4.42, N 7.67; found C 48.45, H 4.51, N 7.53.

[Rh(CO)(2d)Cl] (3d): Yield 0.17 g, 92%; light-brown powder; m.p. 207–208 °C (dec.). IR (KBr): $\tilde{\nu}$(CO) = 2025 cm^{-1}. Elemental analysis for $C_{20}H_{23}ClN_4O_2PRh$ (520.0): calcd. C 46.13, H 4.45, N 10.76; found C 46.29, H 4.33, N 10.61.

[Rh(CO)(2e)Cl] (3e): Yield 0.17 g, 90%; brown powder; m.p. 186–188 °C (dec.). ^{13}C NMR ($CDCl_3$): δ_C = 152.9 (CH=N), 140.9, 128.8, 127.8, 127.5 (all C_{Ph}), 131.5 (d, ^2J = 16.0 Hz), 126.4 (d, ^2J = 4.4 Hz), 114.4, 110.5 (d, $^3J_{C,P}$ = 9.2 Hz) (all C_{Pyr}), 123.1 (d, ^2J = 10.4 Hz, CHNP), 122.9 (d, ^2J = 10.4 Hz, CHNP), 114.0 (d, ^3J = 5.6; *C*HCHNP), 113.9 (d, ^3J = 6.4 Hz, CH*C*HNP), 63.9 (CHN), 21.1 (CH_3). IR (KBr): $\tilde{\nu}$(CO) = 2010 cm^{-1}. Elemental analysis for $C_{22}H_{21}ClN_4OPRh$ (526.0): calcd. C 50.16, H 4.02, N 10.64; found C 50.32, H 3.93, N 10.51.

Palladium Complexes

[Pd(2a)(allyl)]$^+$BF$_4^-$ (4a): Yield 0.25 g, 90%; red powder; m.p. 170–172 °C (dec.). MS (FAB): *m*/*z* (%): 622 (100) [M – BF_4]$^+$, 581 (8) [M – BF_4 – allyl]$^+$, 409 (22). Elemental analysis calcd. (%) for $C_{28}H_{35}BF_4FeN_3OPPd$ (709.1): C, 47.39; H, 4.97; N, 5.92; found: C, 47.57; H, 6.08; N, 6.11.

[Pd(2b)(allyl)]$^+$BF$_4^-$ (4b): Yield 0.21 g, 88%; light-brown powder; m.p. 162–164 °C (dec.). MS (FAB): *m*/*z* (%): 500 (100) [M – BF_4]$^+$, 459 (17) [M – BF_4 – allyl]$^+$, 287 (47). Elemental analysis for $C_{22}H_{25}BF_4N_3O_2PPd$ (587.1): calcd. C 44.96, H 4.29, N 7.15; found C 45.21, H 4.41, N 7.29.

[Pd(2c)(allyl)]$^+$BF$_4^-$ (4c): Yield 0.22 g, 91%; deep-orange powder; m.p. 169–171 °C (dec.). MS (FAB): *m*/*z* (%): 528 (100) [M – BF_4]$^+$, 487 (9) [M – BF_4 – allyl]$^+$, 315 (95). Elemental analysis for $C_{24}H_{29}BF_4N_3O_2PPd$ (615.1): calcd. C 46.82, H 4.75, N 6.82; found C 47.05, H 4.62, N 6.69.

[Pd(2d)(allyl)]$^+$BF$_4^-$ (4d): Light-brown powder; 0.21 g, 90% yield; m.p. 168–170 °C (dec.). MS (FAB): *m*/*z* (%): 501 (100) [M – BF_4]$^+$, 460 (19) [M – BF_4 – allyl]$^+$, 193 (95). Elemental analysis for $C_{22}H_{28}BF_4N_4OPPd$ (588.1): calcd. C 44.89, H 4.79, N 9.52; found C 45.18, H 4.86, N 9.65.

[Pd(2e)(allyl)]$^+$BF$_4^-$ (4e): Yield 0.21 g, 89%; deep-brown powder; m.p. 173–175 °C (dec.). MS (FAB): *m*/*z* (%): 507 (100) [M – BF_4]$^+$, 466 (24) [M – BF_4 – allyl]$^+$, 199 (97). Elemental analysis for $C_{24}H_{26}BF_4N_4PPd$ (594.1): calcd. C 48.47, H 4.41, N 9.42; found C 48.61, H 4.52, N 9.55.

Catalytic Experiments

Palladium-Catalysed Allylic Sulfonylation of 1,3-Diphenylallyl Acetate with Sodium *p*-Toluenesulfinate: A solution of [Pd(allyl)Cl]$_2$ (0.0037 g, 0.01 mmol) or [$Pd_2(dba)_3$]×$CHCl_3$ (0.0103 g, 0.01 mmol) and the appropriate ligand (0.02–0.04 mmol) in THF (5 mL) was stirred for 40 min. 1,3-Diphenylallyl acetate **5** (0.1 mL, 0.5 mmol) was added to the solution and the reaction mixture was stirred for 15 min. Sodium *p*-toluenesulfinate (0.178 g, 1.00 mmol) was then added and the reaction mixture was stirred for 48 h, quenched with brine (10 mL) and extracted with THF (3×7 mL). The organic layer was washed with brine (2×7 mL) and dried over $MgSO_4$. The solvent was evaporated at reduced pressure (40 Torr). Crystallization of the residue from EtOH followed by desiccation in vacuo (10 Torr, 12 h) gave the product **6** as white crystals. All spectroscopic data of compound **6** were in good agreement with the literature.[32]

Palladium-Catalysed Allylic Alkylation of 1,3-Diphenylallyl Acetate with Dimethyl Malonate: A solution of [Pd(allyl)Cl]$_2$ (0.0037 g, 0.01 mmol) or [$Pd_2(dba)_3$]×$CHCl_3$ (0.0103 g, 0.01 mmol) and the appropriate ligand (0.02 mmol) in THF (5 mL) was stirred for 40 min [alternatively, the appropriate presynthesised complex (0.02 mmol) was dissolved in THF (5 mL)]. 1,3-Diphenylallyl acetate **5** (0.1 mL, 0.50 mmol) was added to the solution and the reaction mixture was stirred for 15 min. Dimethyl malonate (0.10 mL, 0.87 mmol), BSA (0.22 mL, 0.87 mmol), and sodium acetate (0.002 g) were also added. The reaction mixture was stirred for 48 h, diluted with THF (5 mL) and filtered through Celite. The filtrate was evaporated at reduced pressure (40 Torr) giving, after in vacuo desiccation (10 Torr, 12 h), product **7** as a colourless oil solidifying upon standing. All spectroscopic data of compound **7** were in good agreement with the literature.[33]

X-ray Crystallographic Study: Crystallographic data for **3a**, **3c** and **3d** are presented in Table 8. All X-ray diffraction measurements were carried out with a SMART 1000 CCD diffractometer at 100 K. The frames were corrected for absorption by the SADABS program.[34]

The principal experimental and crystallographic parameters are presented in Table 8. The structures of **3a**,**c**,**d** were solved by direct methods and refined by full-matrix techniques against F^2 in anisotropic approximations using the SHELXTL 5.1 program package.[35] The positions of hydrogen atoms were calculated geometrically and included in refinement in the rigid body approximation. The absolute configuration of **3a**,**c**,**d** was determined by using the Flack parameter. CCDC-261125 (for **3a**), -261126 (for **3c**) and -261124 (for **3d**) contain supplementary crystallographic data for this paper. These data can be obtained free of charge at www.ccdc.acm.ac.uk/retrieving.html or from the Cambridge Crystallographic Data Centre 12, Union Road, Cambridge CB2 1EZ, UK [Fax: +44-1223-336033].

Acknowledgments

The authors thank Dr. P.V. Petrovskii (Institute of Organoelement Compounds, Moscow) for assistance in characterising the products and Dr. A.V. Korostylev (Leibniz-Institut für Organische Katalyse an der Universitat Rostock, Germany) for assistance in preparation of the manuscript. The authors gratefully acknowledge receiving the chiral HPLC columns (*R*,*R*) WHELK-01 from Regis Technologies (USA) and Chiralcel OD-H from Daicel Chemical Industries,

Table 8. The principal experimental and crystallographic parameters of structures **3a**, **3c** and **3d**.

	3a	**3c**	**3d**
Molecular formula	$C_{26}H_{30}ClFeN_3O_2PRh$	$C_{22}H_{24}ClN_3O_3PRh$	$C_{20}H_{23}ClN_4O_2PRh$
Formula mass	641.71	547.77	520.75
Colour	red	red	yellow
Dimension [mm]	0.40×0.10×0.10	0.50×0.05×0.05	0.20×0.10×0.10
Crystal system	orthorhombic	orthorhombic	orthorhombic
Space group	$P2_12_12_1$	$P2_12_12_1$	$P2_12_12_1$
a [Å]	8.448(3)	9.734(3)	8.704(2)
b [Å]	13.009(5)	10.459(3)	10.883(3)
c [Å]	24.601(9)	23.548(7)	23.190(6)
V [Å^3]	2703.7(17)	2397.3(13)	2196.8(10)
Z	4	4	4
$\rho_{calcd.}$ [g/cm^3]	1.576	1.518	1.575
Temperature [K]	120	293	120
Min./max. 2Θ [°]	1.77/30.00	1.73/29.96	2.07/30.02
Scan type	ω	ω	ω
Radiation, λ(Mo-K_α) [Å]	0.71073	0.71073	0.71073
Linear absorption (μ) [cm^{-1}]	13.33	9.18	9.95
$T_{min.}/T_{max.}$	0.8782/0.6177	0.9555/0.6568	0.9070/0.8258
F(000)	1304	1112	1056
Total refl. (R_{int})	21171 (0.0219)	28694 (0.0369)	17056 (0.0309)
Number of independent reflections	7594	6928	6391
Number of independent refl. with $I > 2\sigma(I)$	6928	5792	6008
Parameters	318	280	264
wR_2	0.0785	0.0479	0.0892
R_1 [for reflections with $I > 2\sigma(I)$]	0.0306	0.0271	0.0329
GOF	0.996	0.990	1.025
Flack parameter	–0.032(16)	–0.031(18)	–0.04(2)
$\rho_{max.}/\rho_{min.}$, [e/Å^3]	1.676/–0.407	0.530/–0.241	1.925/–1.120

Ltd. (Japan). This work was partially supported by the Russian Foundation for Basic Research (Grant No. 03-03-32181) and Grant of the President of RF for young scientists – doctors of sciences (No. MD -21.2003.03).

[1] K. G. Moloy, J. L. Petersen, *J. Am. Chem. Soc.* **1995**, *117*, 7696–7710.
[2] S. Serron, S. P. Nolan, K. G. Moloy, *Organometallics* **1996**, *15*, 4301–4306.
[3] A. Huang, J. E. Marcone, K. L. Mason, W. J. Marshall, K. G. Moloy, S. Serron, S. P. Nolan, *Organometallics* **1997**, *16*, 3377–3380.
[4] A. M. Trzeciak, T. Glowiak, R. Grzybek, J. J. Ziolkowski, *J. Chem. Soc., Dalton Trans.* **1997**, 1831–1838.
[5] S. Serron, J. Huang, S. P. Nolan, *Organometallics* **1998**, *17*, 534–539.
[6] T. S. Barnard, M. R. Mason, *Organometallics* **2001**, *20*, 206–214.
[7] A. D. Burrows, R. W. Harrington, M. F. Mahon, M. T. Palmer, F. Senia, M. Varrone, *J. Chem. Soc., Dalton Trans.* **2003**, 3717–3726.
[8] J. Castro, A. Moyano, M. A. Pericas, A. Riera, M. A. Maestro, J. Mahia, *Organometallics* **2000**, *19*, 1704–1712.
[9] R. Jackstell, H. Klein, M. Beller, K.-D. Wiese, D. Rottger, *Eur. J. Org. Chem.* **2001**, 3871–3877.
[10] S. C. van der Slot, J. Duran, J. Luten, P. C. J. Kamer, P. W. N. M. van Leeuwen, *Organometallics* **2002**, *21*, 3873–3883.
[11] E. E. Nifantyev, A. V. Shishin, A. T. Teleshev, A. R. Bekker, N. N. Nevskii, N. N. Baturin, *Russ. J. Gen. Chem.* **1991**, *61*, 2481–2493.
[12] P. S. Pregosin, R. W. Kunz, in: *^{31}P NMR and ^{13}C NMR of Transition Metal Phosphine Complexes* (in series NMR Basic Principles and Progress), Springer Verlag: New York, **1979**, p. 16.
[13] C. Reichardt, in: *Solvents and Solvent Effects in Organic Chemistry*; VCH Verlagsgesellschaft: Weinheim, **1988**, p. 141.
[14] W. Simanko, K. Mereiter, R. Schmid, K. Kirchner, A. M. Trzeciak, J. J. Ziolkowski, *J. Organomet. Chem.* **2000**, *602*, 59–64.
[15] J. Ansell, M. Wills, *Chem. Soc. Rev.* **2002**, *31*, 259–268.
[16] O. Molt, T. Schrader, *Synthesis* **2002**, 2633–2670.
[17] K. N. Gavrilov, O. G. Bondarev, A. I. Polosukhin, *Russ. Chem. Rev.* **2004**, *73*, 671–700.
[18] K. N. Gavrilov, O. G. Bondarev, R. V. Lebedev, A. A. Shiryaev, S. E. Lyubimov, A. I. Polosukhin, G. V. Grintselev–Knyazev, K. A. Lyssenko, S. K. Moiseev, N. S. Ikonnikov, V. N. Kalinin, V. A. Davankov, A. V. Korostylev, H.-J. Gais, *Eur. J. Inorg. Chem.* **2002**, 1367–1376.
[19] K. N. Gavrilov, *Russ. J. Inorg. Chem.* **1997**, *42*, 368–384.
[20] A. I. Polosukhin, O. G. Bondarev, S. E. Lyubimov, A. V. Korostylev, K. A. Lyssenko, V. A. Davankov, K. N. Gavrilov, *Tetrahedron: Asymmetry* **2001**, *12*, 2197–2204.
[21] O. G. Bondarev, S. E. Lyubimov, A. A. Shiryaev, N. E. Kadilnikov, V. A. Davankov, K. N. Gavrilov, *Tetrahedron: Asymmetry* **2002**, *13*, 1587–1588.
[22] K. N. Gavrilov, V. N. Tsarev, A. A. Shiryaev, O. G. Bondarev, S. E. Lyubimov, E. B. Benetsky, A. A. Korlykov, M. Yu. Antipin, V. A. Davankov, H.-J. Gais, *Eur. J. Inorg. Chem.* **2004**, 629–634.
[23] A. J. Deeming, I. P. Rothwell, M. B. Hursthouse, K. M. Abdul Malik, *J. Chem. Soc., Dalton Trans.* **1980**, 1974–1982.
[24] A. D. Burrows, M. F. Mahon, M. Varrone, *J. Chem. Soc., Dalton Trans.* **2003**, 4718–4730.
[25] J. A. McCleverty, G. Wilkinson, *Inorg. Synth.* **1966**, *8*, 211–214.
[26] P. R. Auburn, P. B. McKenzie, B. Bosnich, *J. Am. Chem. Soc.* **1985**, *107*, 2033–2046.
[27] K. Moseley, P. M. Maitlis, *J. Chem. Soc., Dalton Trans.* **1974**, 169–175.
[28] H. Yang, M. A. Khan, K. M. Nicholas, *Organometallics* **1993**, *12*, 3485–3494.
[29] H. Brunner, B. Habler, *Z. Naturforsch., Teil B* **1998**, *53*, 476–480.
[30] H. Brunner, B. Reiter, G. Riepl, *Chem. Ber.* **1984**, *117*, 1330–1354.
[31] K. N. Gavrilov, O. G. Bondarev, R. V. Lebedev, A. I. Polosukhin, A. A. Shiryaev, S. E. Lyubimov, P. V. Petrovskii, S. K. Moiseev, V. N. Kalinin, N. S. Ikonnikov, V. A. Davankov, A. V. Korostylev, *J. Organomet. Chem.* **2002**, *655*, 204–217.
[32] D. Seebach, E. Devaquet, A. Ernst, M. Hayakawa, F. N. M. Kuhlne, W. B. Schweizer, B. Weber, *Helv. Chim. Acta* **1995**, *78*, 1636–1645.
[33] S. Breeden, M. Wills, *J. Org. Chem.* **1999**, *64*, 9735–9738.
[34] G. M. Sheldrick, *SADABS*, v.2.01, Bruker/Siemens Area Detector Absorption Correction Program, Bruker AXS, Madison, Wisconsin, USA.
[35] G. M. Sheldrick, *SHELXTL-97*, V5.1, Bruker AXS Inc., Madison, WI 53719, USA, **1997**.

Received: January 24, 2005
Published Online: July 6, 2005

